Spatiotemporal Evolution of Ecological Resilience in the Yangtze River Basin and Its Response to Extreme Climate

Yongsi Luo*

School of Resources and Environmental Engineering, Wuhan University of Technology, Wuhan 430070, China

Abstract: Under global warming, frequent extreme climate events threaten ecosystem stability. Clarifying the spatiotemporal evolution of ecological resilience and its response to climate stress is crucial for ecological management. Using multi-source data from 2000 to 2024, the study constructed an ecological resilience evaluation system, employed Theil-Sen trend analysis, M-K test, and a two-way fixed effects model to reveal resilience patterns in the Yangtze River Basin and differential responses of land cover types to extreme climate. The results show that: (1) Ecological resilience exhibits higher values in the south, with an overall increasing trend. The Sichuan Basin and middle-lower plain show significant improvement, the Qinghai source region shows recovery, and the lower Jinsha River shows degradation. (2) Extreme climate displays an increasing trend in the west but decreasing in the east, spatially coupled with resilience changes. (3) Response to extreme climate differs fundamentally among land cover types: forest demonstrates high resistance but slow recovery, with lagged negative effects from high temperature; grassland exhibits low resistance but fast recovery and is sensitive to moisture changes. (4) Extreme precipitation positively buffers cropland and built-up areas in the current period but shows significant lagged negative effects. The response of ecological resilience to climate change exhibits significant lag effects and varies by land cover type, necessitating tailored enhancing strategies.

1 Introduction

Global warming intensifies the frequency and severity of extreme climate events, challenging ecosystems[1]. As an ability to resist interference, maintain balance, and recover, ecological resilience (ER) is the key to measuring ecological security[2]. Under the background of normalization and compounding of extreme climate events, quantifying the spatiotemporal evolution of ecological resilience and its response to climate stress is essential for adaptive management[3].

Existing studies use single indicators like Gross Primary Production (GPP)[4] or Normalized Difference Vegetation Index (NDVI)[5], reflecting immediate vegetation activity but failing to capture structural stability, service maintenance, and recovery potential. This obscures differentiated response patterns and biases risk identification. Additionally, ecological responses show significant lag effects[6]; current resilience results from both historical and contemporary stresses. Thus, composite ER indicators by land cover type are needed. Methodologically, correlation analysis, linear trends, or machine learning cannot strictly control for inherent regional attributes and time-varying factors. A two-way fixed effects model is needed to isolate net climate effects and lag characteristics[7].

This study constructed an ER system encompassing resistance, recovery, and adaptability using 2000–2024 multi-source data, analyzed ER spatiotemporal evolution in the Yangtze River Basin, and employed a two-way fixed effects model to decipher response differences and lag characteristics across land cover types to extreme climate, providing a scientific basis for ecological management.

2 Materials and methods

2.1 Study area

The Yangtze River basin, lying in the climatically sensitive East Asian monsoon zone, features superior hydrothermal conditions but high spatial and temporal heterogeneity. This complexity is compounded by its intricate topography and increasing extreme climatic events. Figure 1 illustrates the diversified land use pattern of forest, cropland, grassland, and impervious surfaces in the basin, providing an ideal setting for exploring resilience differentiation and varied responses to extreme climate events.

2.2 Data sources and processing

Geospatial data originated from multi-source remote sensing products. Fractional vegetation cover came from the National Tibetan Plateau Data Center. Impervious surface information was extracted from the GAIA dataset. Land cover data used CLCD2025; landscape pattern indices were calculated using Fragstats 4.2. NPP data came from MOD17A3HGFV6.1. Topographic data used NASADEM. Meteorological data came from ERA5-Land. An annual panel dataset (2000–2024) was constructed and

* Corresponding author: 348689@whut.edu.cn

resampled to 10 km × 10 km resolution.

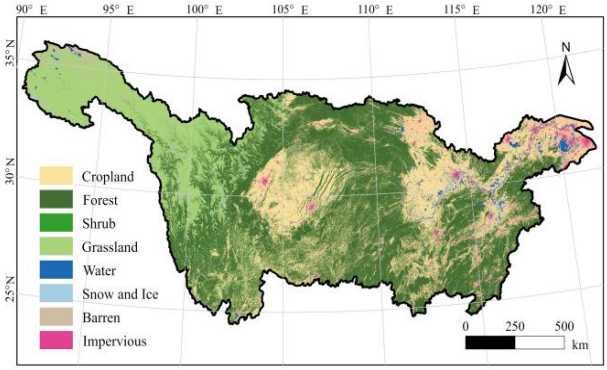

Fig. 1. Land use and land cover classification across the Yangtze River Basin

2.3 Research methods

2.3.1 Evaluation system of ecological resilience

Table 1 shows the ecological resilience evaluation system. Weights were determined using the entropy weight method.

Table 1. Evaluation indices system of ecological resilience

Index	Meaning	Direction	Weight
FVC	Maximum growing season vegetation coverage.	+	0.1451
ISA	Impervious surface proportion per grid, reflecting regional hardening.	-	0.0181
TPI	Relative elevation position, influencing energy redistribution and ecological processes.	+	0.1437
AC	Mean of Aggregation and Contagion indices, reflecting function maintenance.	+	0.0421
SHDI	Landscape patch type richness and evenness, representing structural complexity.	+	0.1778
PD	Patch density, measuring landscape spatial integrity and connectivity.	-	0.0222
Q_w	Capacity to intercept, store and regulate water resources through hydrological processes.	+	0.1211
Q_s	Efficiency in mitigating soil erosion and maintaining fertility.	+	0.1628
Q_c	Capacity to fix and store CO_2 through photosynthesis..	+	0.1671

2.3.2 Entropy Weight TOPSIS method

The Entropy Weight TOPSIS method quantitatively assessed ER[8]. Through standardization, entropy weighting, and identification of positive/negative ideal solutions, relative closeness was calculated as ER.

2.3.3 Extreme climate event identification

Extreme climate (EC) events were identified using percentile thresholds. Daily maximum temperatures exceeding the 90th percentile were classified as extreme high temperature (EH) events, daily precipitation exceeding the 90th percentile as extreme precipitation (EP) events, and daily precipitation below the 10th percentile as extreme drought (ED) events. Extreme warm-wet (EWW) and warm-dry (EWD) events were defined based on temporal combinations: EWW events occurred when an EP event was preceded by EH within three days, while EWD events occurred when EH occurred within three days prior to a day without precipitation. The annual cumulative frequency of each event type per pixel is calculated to construct extreme climate frequency indices.

2.3.4 Spatiotemporal evolution trend analysis

Theil-Sen Median trend analysis combined with the Mann-Kendall significance test revealed long-term evolution of ER and EC. Slope represents trends; the M-K statistic Z determines significance.

2.3.5 Two-way fixed effects model

A two-way fixed effects model incorporating lag terms, isolated dynamic impacts, and lag effects of extreme climate on ER. Individual fixed effects controlled for time-invariant heterogeneity; time fixed effects eliminated macroscopic common trends.

$$ER_{it} = \beta_0 + \beta_{k,0} EC_{it} + \beta_{k,1} EC_{it-1} + \beta_{k,2} EC_{it-2} + \mu_i + \lambda_t + \varepsilon_{it}$$

Where, i represents the pixel, t represents the year (2000-2024), and k refers to a specific type of extreme climate indicator EC (EH, EP, ED, EWW, EWD); ER_{it} is the ecological resilience of pixel i in year t; EC_{it}, EC_{it-1}, and EC_{it-2} represent the extreme climate indicators for the current period, lagged by one year, and lagged by two years, respectively; β_0 is the intercept term; μ_i is the individual fixed effect, controlling for time-invariant heterogeneity factors such as topography and soil; λ_t is the time fixed effect, controlling for macro-climatic fluctuations; ε_{it} is the random error term; the coefficients$\beta_{k,0}$, $\beta_{k,1}$, $\beta_{k,2}$ reflect the immediate effect and cumulative lag effects of extreme climate, representing the net impact of a change in the k-th climate, holding other climate conditions constant and excluding the inherent characteristics of the region.

3 Results and analysis

3.1 Spatiotemporal differentiation of ER and EC

ER spatial distribution showed a significant “south high, north low” pattern (Fig. 2a). High value areas were mainly distributed in the lower Jinsha River below Shigu, indicating a good ecological background. However, trend analysis revealed significant degradationin this area during the study period, decreasing by approximately 0.02 per decade ($P<0.05$) (Fig. 2b). Conversely, the source

region above Shigu, despite the lowest average ER, showed significant recovery, fluctuating upward at 0.02/10a. Most significant ER improvements were in the Sichuan Basin, Taihu Lake Basin, and mainstem below Hukou, with growth rates exceeding 0.03/10a. The middle-lower plain maintained high ER with predominantly positive trends.

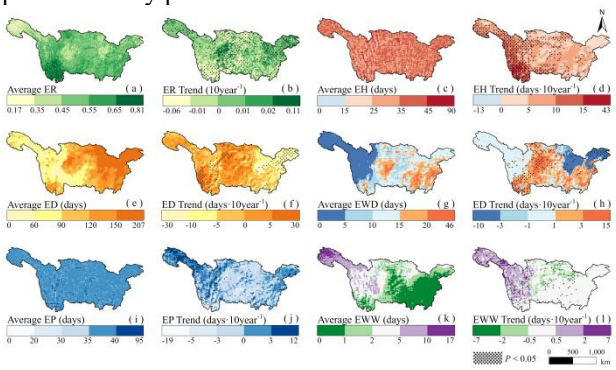

Fig. 2. Spatial distribution of ecological resilience and extreme climate events (a), (c), (e), (g), (i), (k) and their change trends (b), (d), (f), (h), (j), (l)

The western Jinsha River Basin experienced the most drastic climate change, with both EH and EP showing significant increasing trends. ED distribution showed "low west, high east" heterogeneity, with a high value center in the Sichuan Basin (Fig. 2e). Trends showed significant ED alleviation in the mainstem below Hukou and Taihu Lake Basin (Fig. 2f). Intensified EWD areas concentrated in Sichuan, Chongqing, Yunnan, Hubei, Hunan, and Jiangxi (Fig. 2h); significantly increased EWW areas concentrated in the upper Jinsha River (Fig. 2k, l), indicating a warm-wet transition.

ER-EC coupling exhibited significant spatial heterogeneity. The source region showed low ER background recovering under warm-wet conditions, while the lower Jinsha River below Shigu faced high ER background degrading under intensifying warm-dry conditions. The Sichuan Basin demonstrated the most significant recovery rate despite low ER background and high-frequency drought. The middle-lower plain maintained high ER background with continuous enhancement under alleviated warm-dry trends. These differences indicate ecosystem responses are constrained by inherent land cover type and habitat conditions, with climate impacts showing time lags and cross-period accumulation. Thus, econometric models considering lag effects and group regressions by land use type are needed to analyze response differences.

The spatial pattern of ecological resilience in the Yangtze River Basin, characterized by higher values in the south and lower values in the north, fundamentally results from the interplay between hydrothermal conditions and land cover. In high-altitude cold-limited ecosystems, warming effectively extends the vegetation growing season, and coupled with increased precipitation, alleviates physiological water stress during freeze-thaw cycles, thereby significantly enhancing vegetation coverage and carbon sequestration services. Conversely, the ecological resilience degradation risk in the lower Jinsha River is closely associated with its unique dry-hot valley geomorphology and the concurrent 'warming and drying' trend. In water-limited regions, rising temperatures exacerbate soil water deficits. Although deep-rooted trees can sustain themselves by accessing deep soil water, prolonged compound warm-dry stress disrupts stomatal conductance, inhibits vegetation growth, and impairs ecosystem services.

3.2 ER response differences to EC by land cover type

Group modeling was conducted on four dominant land use types: forest, cropland, grassland, and impervious areas (covering >95% of the study area). All continuous variables were Z-score standardized before model construction. Regression results demonstrated significant heterogeneity in ER response to extreme climate among land use types. Figure 3 shows standardized coefficients for the current period, lagged 1 period, and lagged 2 periods (all significant at 95% confidence). Standardized coefficient β reflects immediate and cumulative lag effects.

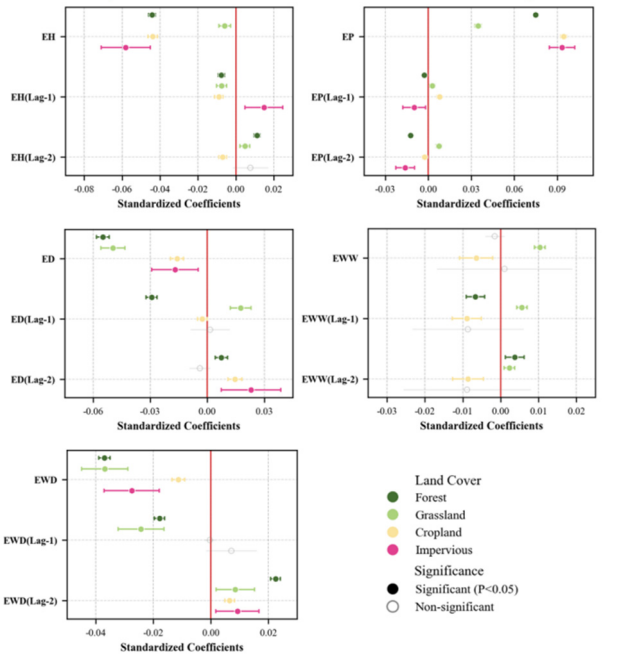

Fig. 3. Forest plot of standardized coefficients of extreme climate events on ecological resilience

Extreme heat (EH) had the greatest impact on impervious areas (β=-0.058): one standard deviation increase in EH frequency decreased built-up area ER by over 0.05 standard deviations, reflecting urban heat island and heatwave effects. Forest and cropland followed (β=-0.044); grassland was the least affected (β=-0.006). Forest showed a significant lagged negative effect (β=-0.008), indicating persistent hindrance.

Extreme precipitation (EP) positively promoted most land cover types in the current period, with cropland (β=0.095) and impervious areas (β=0.093) showing the strongest effects. However, lagged effects rapidly decayed or turned negative, revealing EP primarily induces "immediate buffering" resilience.

Extreme drought (ED) suppressed natural vegetation,

suppressing both forest (β=-0.055) and grassland (β=-0.050). While forests demonstrated high resistance by buffering the immediate impact, they suffered from low recovery and sustained damage. In contrast, grasslands exhibited low resistance with immediate sensitivity but showed a strong capacity for high recovery, as evidenced by a significantly positive lag-one coefficient (β=0.018), indicating rapid compensatory regeneration. Cropland and impervious areas were less sensitive, with cropland displaying a positive rebound at lag-two (β=0.015), possibly related to crop rotation.

Compound events showed more complex impacts. EWD consistently damaged forest and grassland (*β*=-0.037), a key factor in natural vegetation degradation. EWW impact was weak and differentiated: positive for grassland (*β*=0.010), but negative for cropland (*β*=-0.006) and forest with lag (*β*=-0.007), reflecting differential responses to hydrothermal matching.

Future ER management requires spatial zoning. For the lower Jinsha River degradation risk area, enhance drought-tolerant vegetation and soil conservation. For the Qinghai-Tibet Plateau source region, prioritize protection and restoration, leveraging warm-wet windows. The middle-lower plain requires strengthened farmland drainage and sponge city construction to mitigate heat island effects. For instance, although grasslands experience rapid biomass loss during stress, their regenerative capacity exceeds that of forests once hydrothermal conditions improve, owing to the advantages of their belowground bud bank and short life cycle. The positive effect of extreme warm-wet events on grassland aligns with the rapid growth of alpine meadows under favorable conditions. Therefore, in future ecological restoration, vegetation types should be selected based on regional climate risk characteristics. In areas with frequent warm-wet events, grassland may offer greater long-term stability than forest.

4 Conclusion

Based on entropy weight-TOPSIS and two-way fixed effect model, this study systematically evaluated the evolution characteristics of ecological resilience and its response to extreme climate events in the Yangtze River basin from 2000 to 2024, and mainly drew the following conclusions:

(1) ER in the basin displays a distinct spatial pattern, generally higher in the south and lower in the north, with an overall increasing trend of 0.03 per decade. Notable ER improvement was observed in the Sichuan Basin and the middle-lower plain, while the Qinghai source region showed signs of recovery. Conversely, significant ER degradation was detected in the lower Jinsha River.

(2) EC exhibited a trend of increasing intensity in the west and decreasing intensity in the east, which was coupled with the ER changes. The western basin experienced rising temperatures and precipitation surges, whereas drought conditions in the east were alleviated.

(3) Land use types shape differentiated ER response mechanisms. Specifically, forests exhibit high resistance but slow recovery. Grasslands demonstrate low resistance yet rapid regenerative capacity. Croplands show a strong short-term response to EP but possess weak long-term adaptation. Impervious surfaces are particularly sensitive to extreme high temperatures EH.

(4) The two-way fixed effects model confirms that extreme climate impacts exhibit lag effects of one to two years. Specifically, EWW enhances grassland ER while inhibiting forest and cropland ER. These findings suggest that future management strategies should be tailored to local conditions and based on zoning approaches for disaster reduction.

References

1. Lian X, Li Y M K, Liu J G, Kornhuber K, Gentine P. Northern ecosystem productivity reduced by Rossby-wave-driven hot-dry conditions. Nature Geoscience, 2025, 18(7): 615-623.
2. Falk D A, van Mantgem P J, Keeley J E, Gregg R M, Guiterman C H, Tepley A J, Young D J N, Marshall L A. Mechanisms of forest resilience. Forest Ecology and Management, 2022, 512: 120129.
3. Zhang S B, Lei J, Tong Y J, Zhang X L, Lu D N, Fan L Q, Duan Z L. Temporal and spatial responses of ecological resilience to climate change and human activities in the economic belt on the northern slope of the Tianshan Mountains, China. Journal of Arid Land, 2023, 15(10): 1245-1268.
4. Zhang Y L, Song C H, Hwang T, Novick K, Coulston J W, Vose J, Dannenberg M P, Hakkenberg C R, Mao J F, Woodcock C E. Land cover change-induced decline in terrestrial gross primary production over the conterminous United States from 2001 to 2016. Agricultural and Forest Meteorology, 2021, 308: 108609.
5. Wu X Y, Zhu X F. Differential analysis of vegetation response to extreme clinate in diferent vegetation regions of China. Acta Ecologica Sinica,2023,43(24):10202-10215.
6. Kannenberg S A, Schwalm C R, Anderegg W R L.Ghosts of the past: how drought legacy effects shape forest functioning and carbon cycling. Ecology Letters, 2020, 23(5): 891-901.
7. Asmare F, Tabe-Ojong M P J. Climate-smart agriculture and climate resilience: panel data evidence from Ethiopia. Climatic Change, 2025, 178(11): 208.
8. Yang L, Xu Y, Zhu J Q, Sun K Y. Assessment of water ecological resilience and influencing factors in urban agglomerations along the midlle reaches of the Yangtze River. Joumal of Safety and Environment, 2025, 25(1): 335 -347.